Out-of-plane stability of gusset plates using a simplified notional load yield line method

B. Zaboli & G.C. Clifton

Department of Civil and Environmental Engineering, University of Auckland, Auckland.

K. Cowie

Steel Construction New Zealand, Auckland.

2017 NZSEE Conference

ABSTRACT: Gusset plates are a key component of braced frame systems, connecting the braces to the framing system. With traditional concentrically braced frames (CBFs), the braces are designed for controlled inelastic action, which involves brace buckling when the brace is in compression. To avoid the undesirable effects of brace buckling, buckling restrained braces (BRBs) have been developed. BRBs allow a brace to yield in compression without global buckling, thus making the brace of similar stiffness and strength in tension and compression. Testing on individual braces has demonstrated that BRBs can perform very well, however the brace can also fail prematurely if its connections are not appropriately designed and buckle before the brace core yields in compression. Despite the importance of gusset plates, their behaviour has not been well researched, with engineers using a design method originally proposed by Thornton (1984). This is a column analogy used to describe plate behaviour and a number of recent studies have shown that while this method is too conservative in CBF connections, is not reliable in buckling restrained brace frame (BRBF) connections. In this paper, a simplified notional load yield line model is proposed for both CBF and BRB systems, which can adequately take into account the actual collapse mechanisms of brace to frame connections, ensuring gusset plate stability is maintained as required in each system. A comparison of several experimental test results and those of the proposed method is presented showing the method is suitably conservative for application to both CBFs and BRBFs.

1 INTRODUCTION

1.1 Background

Historically, CBFs have been used to resist lateral earthquake loads in steel frame systems. CBFs provide excellent lateral stiffness to prevent damaging story drifts in small to moderate earthquakes, but are not as effective in severe earthquakes due to the system degradation in strength and stiffness from brace bucking in compression. Recent research has led to the development of BRBs to overcome the problems related to buckling of bracing elements. BRBs can dissipate significant hysteretic energy during both tension and compression cycles and allow the building to maintain similar stiffness and develop similar ductility in both directions of cyclic action along a given principal axis.

Gusset plate connections are widely used to connect the diagonals to the framing systems. Due to the complexity of stress distribution, boundary conditions, and geometry in different gusset plate configurations, the stress analysis in the gusset plates is difficult and their actual compressive behaviour is not well known nor easily determined. For design purposes, Thornton proposed a column-based method for predicting the buckling capacity of the gusset plate according to the early research conducted by Whitmore (1952). Gusset plates were considered as rectangular columns with an effective width determined by a 30° stress trajectory (Whitmore width), and the Euler buckling capacity was determined using an effective length factor (K-factor) of 0.65 and the average buckling length (Figure 1).

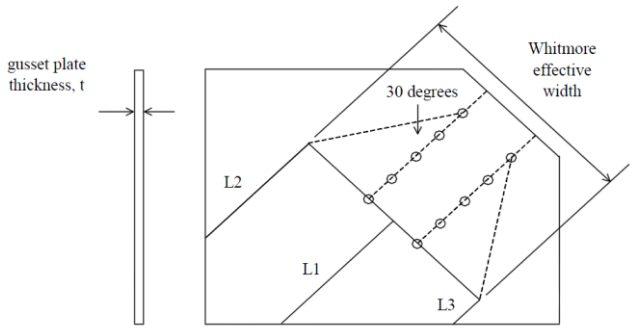

Figure 1. Geometry of Thornton equivalent column (Whitmore 1952).

In the most CBF connections, the Thornton method is conservative because it does not consider the plate action and the out-of-plane restraint provided by the plate outside the boundaries of the effective width. Gross (1990) carried out full-scale tests on braced frame subassemblages and noted that the Thornton method, even with a K-factor of 0.5, could considerably underestimate the actual buckling capacity of the gusset plates. Higgins et al. (2013) tested six large-scale gusset plate specimens representing the I-35W Mississippi River Bridge, which collapsed due to buckled gusset plates, and indicated that the largest experimental K-factor was 0.8 and K-factors less than unity can be applied to estimate the compressive capacity of gusset plates that buckle in a sway mode. As an important observation, all six specimens failed by sway buckling mode under the yield-line (Figure 2(a)). Yam & Cheng (2002) reported thirteen full-scale tests, and it was also deduced that, owing to stress redistribution in corner gusset plates, using a stress trajectory angle of 30° could be too conservative and a 45° dispersion angle would give a more reasonable prediction of buckling capacity. A more comprehensive approach was suggested by Dowswell (2014) in which a variable stress dispersion angle was formulated to estimate buckling capacity of gusset plates with different configurations and inelastic deformation capacity. Recent research conducted by Dowswell (2016) developed a notional load yield-line (NLYL) model for gusset plate stability that effectively considers many critical parameters that control the compressive behaviour of gusset plates, such as the initial imperfection, yielding of the section, reduction in stiffness, large eccentricity, second-order effect, and plate action. However, this method utilizes a yield-line pattern and buckling length that is not consistent with the experimental observations.

On the other hand, BRBF connections have been identified as a critical area where insufficient research has been undertaken. Currently, engineers employ a method based on the CBF connection behaviour. However, BRBs have different structural characteristics to normal braces which may lead to an instability failure of gusset plates if designed to a method based on CBF connection behaviour. Tsai & Hsiao (2008) and Chou & Liu (2012) tested full-scale BRBFs and reported the out-of-plane buckling of the gusset plate. Consequently, they recommended that the K-factor should be 0.65 and 2, for the cases stiffened and regular gusset plate respectively. However, as can be inferred from Figure 2(b), the tests exhibited a plastic failure mode over the yield-line. Therefore, an increased K-factor would not be the best approach to cover this failure mode.

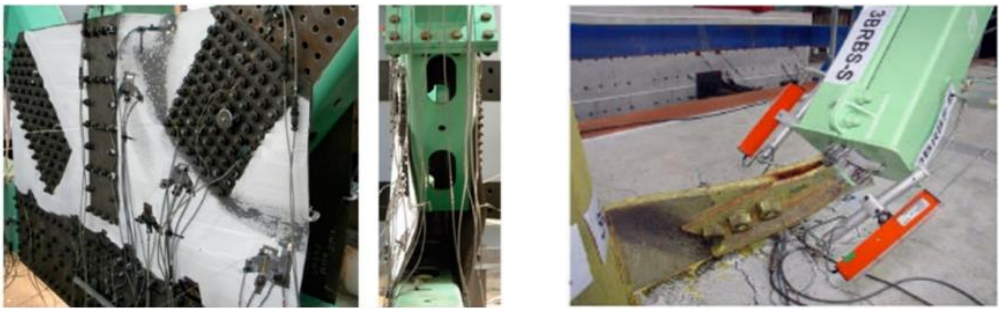

Figure 2. Two different gusset plate failure modes: (a) gusset buckling mode under the yield-line (Higgins et al. 2013); (b) plastic failure mode over the yield-line (Tsai et al. 2008).

In a pioneering study undertaken by Takeuchi et al. (2014), focus was given to the moment transfer

capacity of the restrainer end, and a set of sophisticated equations for BRB stability was developed. Although this method considered many details of the BRB anatomy as well as the rotational stiffness of the gusset plate, in practice obtaining the rotational stiffness of different gusset plate configurations is far from straightforward. It also did not take account of the gusset buckling mode under the yield-line.

1.2 **Current design practice**

The most recent American guidelines such as the AISC Seismic Design Manual (AISC 2012), and the AISC 29 Steel Design Guide (Muir & Thornton 2014) have adopted the Thornton method and by using the AISC column curve, the compressive strength, initial imperfection of $L/1500$, and accidental eccentric loading are considered. The current recommended values for the K-factor are 0.5 for a corner gusset plate, as established by Gross (1990), and 1.2 for a single brace gusset plate that is connected at only one edge. In all cases, the middle length to the nearest support point (L_1) is used as the buckling length. As an alternative, these guidelines reference the K-factors and buckling lengths suggested by Dowswell (2006, 2012) that were calibrated for different gusset configurations to provide more accurate solutions. Similarly, in New Zealand codes of practice, the Thornton method has been applied along with the NZS 3404 (1997) column curve. HERA R4-80 (Clifton 1994) followed the K-factor of 0.5 and the average buckling length by Gross (1990), however, in NZS 3404 the K-factor was changed to 0.7 and applied the clear buckling length that is the middle length.

1.3 **Research objectives**

In view of the above, it can be seen that there is no comprehensive and robust design procedure for gusset plates available, to capture very well the key parameters governing the stability of the systems. This is especially true in BRBFs. The main objective of this study is to develop a practical and more logical design procedure, which can adequately take into account the actual collapse mechanisms of the gusset plates in both CBF and BRBF connections using a simplified notional load yield line model.

2 **PROPOSED DESIGN PROCEDURE**

As a general stability rule, larger initial imperfection means more lateral load and less stability. Thus, the accuracy of a gusset plate buckling capacity approximation would depend on the level of out-of-plane initial imperfection and deformation. The initial imperfection as well as deflection on the gusset that is triggered by the brace end can induce bending moment on the folding line of the gusset and subsequently plastify it when enough strength is not provided. Creation of this hinge line will significantly reduce the elastic buckling capacity of the gusset plate and as a result it may buckle even though it was designed to remain elastic under the prescribed axial load using an effective length calculation method. For this reason, the starting point has to have a reasonable estimate of the in situ out-of-plane imperfection, and then the notional load at the brace end becomes:

$$N = \theta_i N^{\star} \quad (1)$$

$$N = \theta_i N_{cu}^{\star} \quad (2)$$

Where $N =$ notional load at brace end on the yield-line, $\theta_i =$ total initial imperfection angle, $N^{\star} =$ overstrength compression capacity of the brace in CBF, $N_{cu}^{\star} =$ overstrength compression capacity of the core in BRB.

2.1 **Initial imperfection**

In CBFs the initial imperfection is a combination of out-of-plumbness of the brace and out-of-flatness of the gusset plate with the recommended values (Dowswell 2016) of $1/500$ and $1/100$ respectively (Figure 3(a)). In addition, to consider the reduced stiffness of the gusset plate due to the out-of-plane displacement, the out-of-flatness of the gusset plate is magnified by a factor of two (Dowswell 2016):

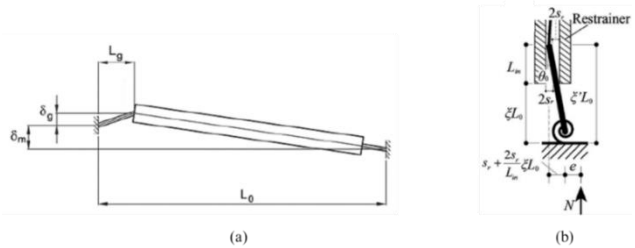

Figure 3. (a) Initial imperfection of CBFs (Dowswell 2016); (b) initial imperfection angle of the insert zone for BRBs (Takeuchi et al. 2014).

$$\theta_i = \frac{\delta_m}{L_0} + \frac{2\delta_g}{L_g} = \frac{1}{500} + \frac{2 \times 1}{100} = 2.2\% \quad (3)$$

Where $\delta_m/L_0 =$ plumbing tolerance of the brace, $\delta_g/L_g =$ out-of-flatness tolerance of the gusset.

If accounted for the simultaneous story out-of-plane drift of 1.2%, the SRSS method can be used:

$$\Rightarrow \theta_i = \sqrt{(2.2)^2 + (1.2)^2} = 2.5\% \quad (4)$$

Designing a brace for 2.5% of the member compressive force is a simple stability bracing requirement that has been used in NZS 3404 and in a number of BRB gusset plate designs to date.

As shown in Figure 3(b), in BRBs the initial imperfection at the insert zone may represent the largest source of imperfection, which is also required to be considered (Takeuchi et al. 2014):

$$\theta_0 = \frac{2S_r}{L_{in}} \quad (5)$$

Where $\theta_0 =$ initial imperfection angle of the insert zone, $S_r =$ clearance between core and restrainer, $L_{in} =$ insert zone length.

Then, the total initial imperfection in BRBs can be approximated by the following equations:

$$\begin{cases} \theta_i = \dfrac{\delta_m}{L_0} + \dfrac{2\delta_g}{L_g} + \theta_0 & \textit{gusset plate buckling mode under the yield-line} \quad (6) \\ \theta_i = \dfrac{\delta_m}{L_0} + \dfrac{\delta_g}{L_g} + \theta_0 & \textit{plastic failure mode over the yield-line} \quad (7) \end{cases}$$

2.2 **Yield-line patterns**

Based on experimental observations, three different patterns of anticipated yield-line are defined. When the brace moves out-of-plane without a plastic hinge at the mid-length of it or at the end of the restrainer in BRBs, the gusset will buckle under the yield-line that runs from the middle of the gusset plate edge to the underside of the brace and back to the middle of the other gusset plate edge (Figure 4(a)). When the brace buckles in out-of-plane direction and forms a plastic hinge at the mid-length of it or at the end of the restrainer in BRBs, plastic failure over the yield-line will occur and the yield-line will run from the corner of the gusset to the underside of the brace and back to the other corner as shown in Figure 4(b). If the brace is not pulled in close to the beam or column, the yield-line will run from the line of restraint that occurs at the first re-entrant corner of the gusset to the gusset plate edge in a straight line and parallel to the end of the brace (Figure 4(c)).

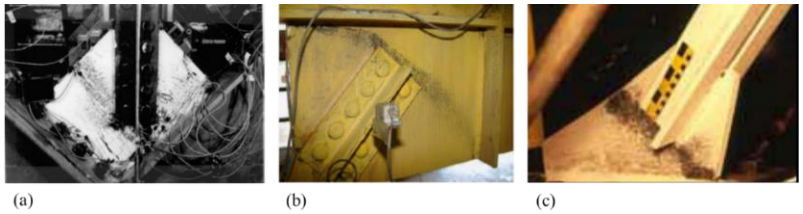

Figure 4. (a) Gusset buckling under the yield-line (Yam & Cheng 2002); (b) plastic failure over the yield-line (interrupted yield-line pattern) (Tsai et al. 2008); (c) plastic failure over the yield-line (uninterrupted yield-line pattern) (Astaneh-Asl et al. 2006).

2.3 **NLYL Model for CBFs**

In CBF connections the system is modelled as a bending element with plastic hinges at the gusset plate. If the bending moment reaches the reduced plastic moment capacity of the gusset including the axial force effect, any further increase in load will cause collapse (Dowswell 2016). According to the simple and very satisfactory plastic analysis, the virtual work method, the stability condition of CBFs is expressed as follows (Figure 5(a)):

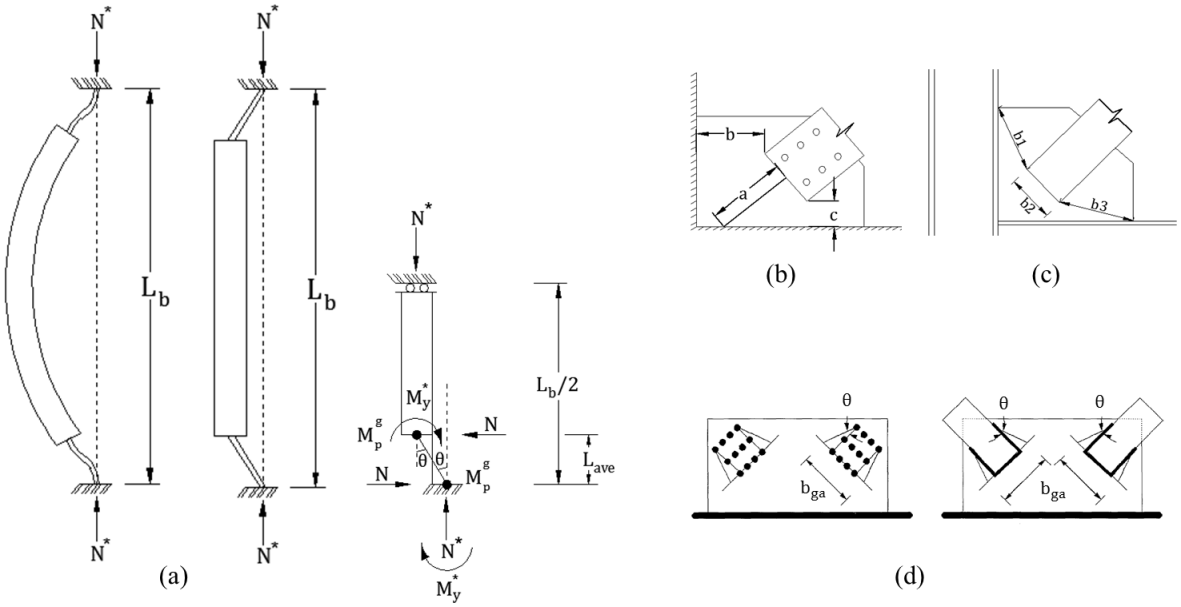

Figure 5. (a) Simplified collapse mechanisms of CBFs; (b) geometry to define the average length, L_{ave}; (c) total yield-line length, b_{gf}; (d) stress distribution within gusset plate for bolted and welded connections (Astaneh-Asl 1998).

$$NL_{ave}\delta_S\theta = 2M_p^g\theta \;\Rightarrow M_p^g \geq \frac{NL_{ave}\delta_S}{2} = M_y^\star \tag{8}$$

Using an L-shaped model, Dowswell (2006) showed that the out-of-plane restraint is provided by the portion of the gusset plate with the shorter length of the two distances from brace end to the supports(c). Considering this observation, the plate length in bending is defined in Figure 5(b) and:

$$L_{ave} = min\begin{cases}(a+c)/2\\(a+b+c)/3\end{cases} \tag{9}$$

$$\delta_S = \frac{1}{1-\frac{N^\star}{N_e}} \geq 1 \tag{10}$$

$$N_e = f_e t_g b_{ga} \tag{11}$$

$$f_e = \frac{\pi^2 E}{\left(\frac{L_{ave}}{r_g}\right)^2} \tag{12}$$

$$IN:\begin{cases}\left(\frac{N^\star}{\phi N_s^g}\right)^2 + \frac{M_y^\star}{\phi M_{sy}^g} \leq 1 & \textit{regular gusset} \quad (13)\\ \left(\frac{N^\star}{\phi N_s^g}\right)^2 + \frac{M_y^\star}{\phi(1.19)M_{sy}^g} \leq 1 & \textit{stiffened gusset} \quad (14)\end{cases}$$

$$N_s^g = t_g b_{ga} f_y \quad (15)$$

$$M_{sy}^g = S_g f_y = \frac{b_{gf} t_g^2}{4} f_y \quad (16)$$

$$b_{gf} = b_1 + b_2 + b_3 \quad (17)$$

Where $\delta_S =$ moment amplification factor to account for second-order effect, $N_e =$ elastic buckling capacity of gusset, $t_g =$ gusset thickness, $b_{ga} =$ effective width in compression as shown in Figure 5(d) (dispersion angle is 40° for corner gusset plates and 30° for other configurations), $E =$ Young's modulus of elasticity, $r_g =$ radius of gyration of gusset, $IN =$ interaction equation from plastic theory for rectangular and weak-axis bending of wide-flange sections respectively, $M_{sy}^g =$ plastic moment capacity of gusset, $N_s^g =$ nominal section axial capacity of gusset, $S_g =$ plastic section modulus of gusset, $f_y =$ yield stress of the gusset, $b_{gf} =$ total length of the yield-line (Figure 5(c)).

2.4 **NLYL Model for BRBs**

In BRB connections the plastic hinges are assumed at both the gusset plate and restrainer end (Takeuchi et al. 2014). Given the fact that at least three hinges are required for the system collapse, the stability conditions of BRBs encompass the following forms (Figure 6):

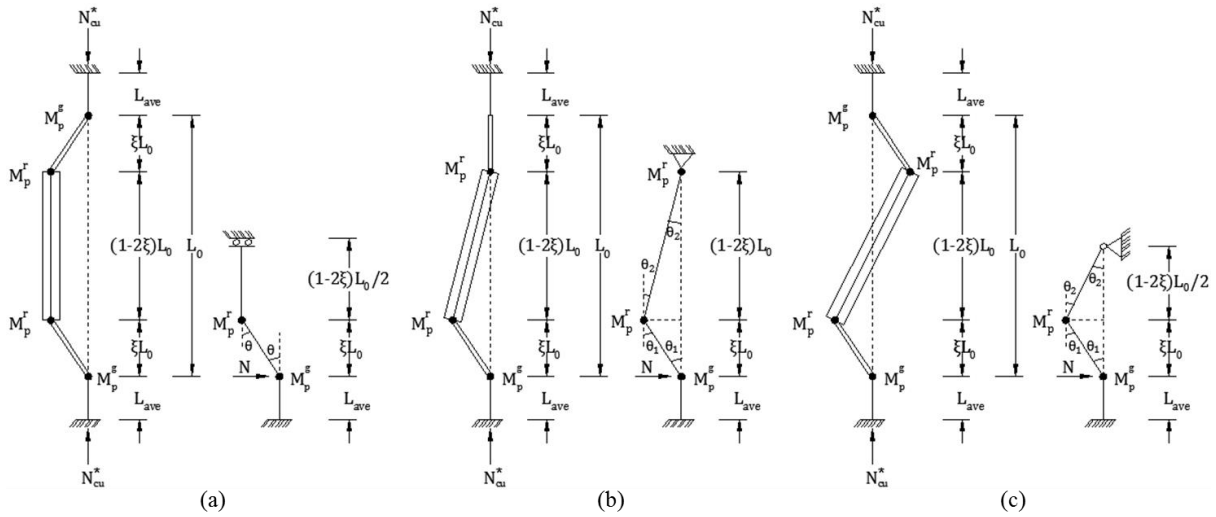

Figure 6. Collapse mechanisms of BRBs for plastic failure over the yield-line mode: (a) symmetrical mode; (b) one sided mode; (c) asymmetrical mode.

Symmetrical mode:

$$N\xi L_0 \delta_S \theta = M_p^g \theta + M_p^r \theta \quad (18)$$

$$N\xi L_0 \delta_S \leq M_p^g + M_p^r \quad (19)$$

One sided mode:

$$N\xi L_0 \delta_S (\theta_1 + \theta_2) = M_p^g \theta_1 + M_p^r (\theta_1 + 2\theta_2) \quad (20)$$

$$N\xi L_0 \delta_S (1 - \xi) \leq (1 - 2\xi)\, M_p^g + M_p^r \quad (21)$$

Asymmetrical mode:

$$N\xi L_0 \delta_S (\theta_1 + \theta_2) = M_p^g \theta_1 + M_p^r (\theta_1 + \theta_2) \quad (22)$$

$$N\xi L_0 \delta_S \leq (1 - 2\xi)\, M_p^g + M_p^r \quad (23)$$

As can be seen, the asymmetrical mode gives the lowest failure capacity and governs stability.

$$\delta_S = \frac{1}{1 - \frac{N_{cu}^{\star}}{N_{cr}^{B}}} \geq 1 \tag{24}$$

$$N_{cr}^{B} = \frac{\pi^2 EI_B}{(kL_0)^2} \longrightarrow \begin{cases} k = 1 & \textit{regular gusset} \\ k = 0.7 & \end{cases}$$
$$N_{cr}^{B} = \frac{\pi^2 EI_B}{(kL_0)^2} \longrightarrow \begin{cases} k = 1 & \textit{stiffened gusset} \\ k = 0.7 & \end{cases} \tag{25}$$

$$M_p^g = \begin{cases} \phi M_{sy}^g \left(1 - \left(\frac{N_{cu}^{\star}}{\phi N_s^g}\right)^2\right) & \textit{regular gusset} \quad (26) \\ 1.19\phi M_{sy}^g \left(1 - \left(\frac{N_{cu}^{\star}}{\phi N_s^g}\right)^2\right) & \textit{stiffened gusset} \quad (27) \end{cases}$$

$$M_p^r = min\left\{ M_p^{r-neck},\ M_p^{r-rest} \right\} \tag{28}$$

$$M_p^{r-neck} = \begin{cases} \phi M_{sy}^n \left(1 - \left(\frac{N_{cu}^{\star} - N_{wy}^n}{\phi\left(N_y^n - N_{wy}^n\right)}\right)^2\right) & \textit{regular gusset} \quad (29) \\ \phi M_{sy}^n \left(1 - \left(\frac{N_{cu}^{\star} - N_{wy}^n}{\phi\left(N_u^n - N_{wy}^n\right)}\right)^2\right) & \textit{stiffened gusset} \quad (30) \end{cases}$$

Where ξL_0 = BRB connection length from the end of restrainer to the yield-line, L_0 = total BRB length, δ_S = moment amplification factor to account for second-order effect, $N_{cu}^{\star}$ = overstrength compression capacity of core in BRB, N_{cr}^{B} = global elastic buckling capacity of BRB including effect of gusset plate, EI_B = bending stiffness of restrainer, M_p^g = reduced plastic moment capacity of gusset plate including axial force effect, M_{sy}^g = plastic moment capacity of gusset, M_p^r = restrainer moment transfer capacity, M_p^{r-neck} = reduced restrainer moment transfer capacity determined by cruciform core plate at the neck including axial force effect, M_{sy}^n = plastic moment capacity of neck, M_p^{r-rest} = restrainer moment transfer capacity determined by restrainer section at rib end, N_{wy}^n = yield axial force of cruciform neck at web zone, N_y^n = yield axial strength of neck, N_u^n = ultimate axial strength of neck, S_n = plastic section modulus at neck.

Takeuchi et al. (2014) also showed that if the insert zone is more than 2.0 times the core plate width, M_p^r is determined by M_p^{r-neck}.

In BRBFs there is also a possibility that gusset plate buckles under the yield-line. In this case, the stability conditions are (Figure 7):

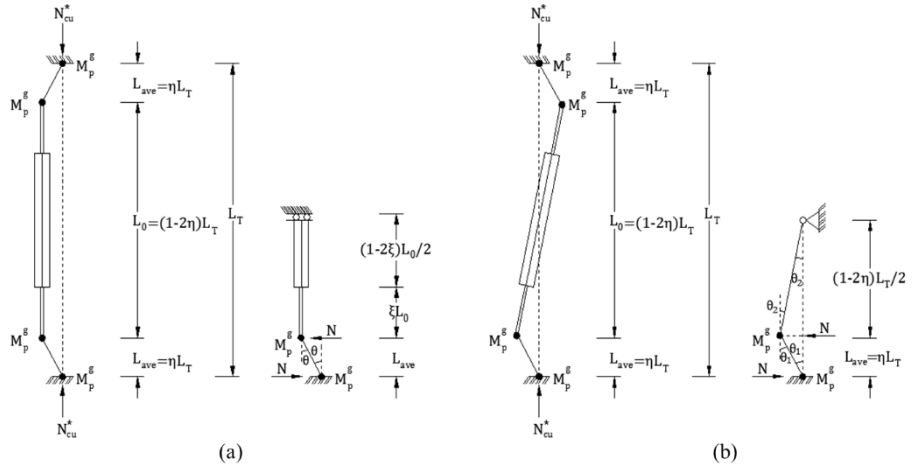

Figure 7. Collapse mechanisms of BRBs for gusset buckling under the yield-line mode: (a) symmetrical mode; (b) asymmetrical mode.

Symmetrical mode:

$$NL_{ave}\delta_S\theta = 2M_p^g\theta \;\Rightarrow M_p^g \geq \frac{NL_{ave}\delta_S}{2} = M_y^\star \tag{31}$$

Asymmetrical mode:

$$NL_{ave}\delta_S = (2-2\eta)\,M_p^g \;\Rightarrow M_p^g \geq \frac{NL_{ave}\delta_S}{(2-2\eta)} = M_y^\star \tag{32}$$

Similarly, the asymmetrical mode gives the lowest failure capacity and governs stability.

3 CHEVRON CONFIGURATION

In a BRBF with chevron configuration, the flexibility of the frame beam and the bending capacity of restrainer end considerably affect the stability of the system (Takeuchi et al. 2016). Hikino et al. (2013) showed that when the insert zone exceeded 1.5 times the width of the core and there was enough moment transfer capacity at the end of restrainer, the BRB exhibited excellent ductility during the shake table tests. Otherwise, to prevent the rotation of the beam in out-of-plane direction the recommended stiffness of the torsional bracing is (Figure 8):

$$K_R \geq 2N_{cu}^\star \frac{L_1(L_1+L_2)}{L_2} \tag{33}$$

If sufficient torsional stiffness is not provided by the beam, it is important that adequate lateral bracing at the midspan of the beam be used. In this case, the BRB connection can be designed using the NLYL method based on the assumption of a single diagonal configuration.

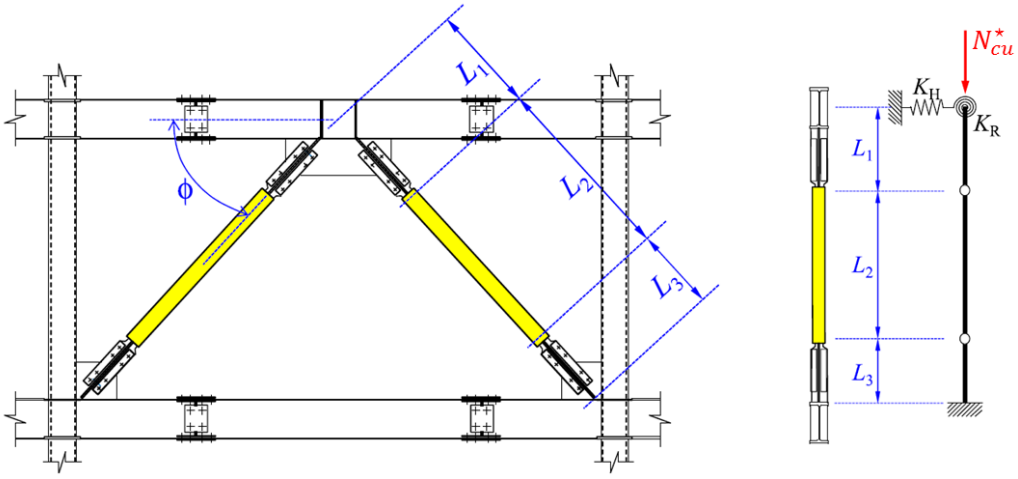

Figure 8. Geometry of chevron configuration (Hikino et al. 2013).

4 COMPARISON TO TEST DATA

4.1 CBF Specimens

Table 1 presents two full-scale CBF test results (Gross 1990) by which the suitability of different methods can be assessed. It can be seen that both the AISC and NZS 3404 methods are too conservative and overdesign the gusset plate. Several past experiments (Lopez et al. 2002; Uriz & Mahin 2008; Palmer et al. 2016) have shown that in-plane stiffness of the gusset plate can have detrimental effects on the seismic performance of a steel braced frame. In a number of these experiences, column and beam hinging or fracture was observed as a result of the generation of a large in-plane bending moment when story undergoes large inelastic drifts. Designing a gusset plate by means of the NLYL method will yield the minimum required thickness and reduce the mobilization of this in-plane stiffness.

Table 1. Comparison of predicted failure axial force in different methods to the physical CBF tests

Specimen	Failure axial force (kN)				
	AISC ($k = 0.5, l_b = l_1$)	NZS 3404 ($k = 0.7, l_b = l_1$)	NLYL	Experiment (Gross 1990)	
				General yield capacity	Ultimate buckling capacity
No. 1	319	221	380	396	516
No. 2	319	221	380	400	614

4.2 **BRB Specimens**

Comparison between different methods and the results from six BRB tests (Takeuchi et al. 2014) is summarized in Table 2. It is observed that the NLYL method produces suitably conservative results, however, neither the AISC nor NZS 3404 can predict the failure axial force conservatively owing to a larger initial imperfection in BRB specimens.

On the other hand, although theoretically the asymmetrical mode governs stability, in some cases it is also possible that a BRB buckles in a mode with higher compressive capacity since the final buckling mode would primarily depend on the initial imperfection shape. This could be one of the sources of conservatism in both the Takeuchi and NLYL methods.

Table 2. Comparison of predicted failure axial force in different methods to the physical BRB tests

Specimen	Failure axial force (kN)					
	Gusset buckling under the yield-line			Plastic failure over the yield-line		Experiment (Takeuchi 2014)
	AISC ($k = 0.5; l_b = l_1$)	NZS 3404 ($k = 0.7; l_b = l_1$)	$NLYL_{gb}$	$NLYL_{pf}$	Takeuchi method	
MRL1.0S1H	620	561	778	725	818	-
MRL2.0S1	620	561	608	436	520	535
MRL2.0S2	620	561	556	367	410	507
MCL2.0S2	620	561	562	385	432	375
MRL1.0S1	620	561	565	326	345	362
MRL1.0S2	620	561	482	207	217	300

* MRL1.0S1H did not fail in experiment

5 **CONCLUSIONS**

A simplified stability design method is proposed in this paper, based on the concept of notional load method, which aims to determine the minimum size of gusset plates necessary to provide the out-of-plane stability condition in actual design. A comparison between the computed results obtained from the NLYL method and the available testing shows that it is suitably conservative and can be used for different gusset plate configurations in both CBFs and BRBFs.

REFERENCES

AISC. (2012). *Seismic design manual (2nd ed.)*. Chicago, IL: American Institute of Steel Construction.

Astaneh-Asl, A. (1998). *Seismic behaviour and design of gusset plates*. (Steel Technical Information and Product Services (Steel TIPS)), Moraga, CA: Structural Steel Educational Council.

Astaneh-Asl, A., Cochran, M.L. & Sabelli, R. (2006). *Seismic detailing of Gusset plates for Special Concentrically braced frames*. (Steel Technical Information and Product Services (Steel TIPS)), Moraga, CA: Structural Steel Educational Council.

Chou, C., & Liu, J. (2012). *Frame and brace action forces on steel corner gusset plate connections in buckling-restrained braced frames*. Earthquake Spectra, 28(2), 531-551.

Clifton, G. C. (1994). *New Zealand structural steelwork limit state design guides volume 1*. (No. R4-80), Manukau City: HERA.

Dowswell, B. (2006). *Effective length factors for gusset plate buckling*. (AISC) Engineering Journal, Second Quarter, 91-101.

Dowswell, B. (2012). *Effective length factors for gusset plates in chevron braced frames.* (AISC) Engineering Journal, Third Quarter, 115-117.

Dowswell, B. (2014). *Gusset plate stability using variable stress trajectories*. (pp. 2629-2639) American Society of Civil Engineers.

Dowswell, B. (2016). *Advances in steel connection analysis*. 2016 NASCC (the Steel Conference Proceedings).

Gross, J. L. (1990). *Experimental study of gusseted connections*. (AISC) Engineering Journal, 3rd Quarter, 89-97.

Higgins, C., Hafner, A., Turan, O. & Schumacher, T. (2013). *Experimental tests of truss bridge gusset plate connections with sway-buckling response*. Journal of Bridge Engineering, 18(10), 980-991.

Hikino, T., Okazaki, T., Kajiwara, K. & Nakashima, M. (2013). *Out-of-plane stability of buckling-restrained braces placed in chevron arrangement*. Journal of Structural Engineering, 139(11), 1812-1822.

Lopez, W.A., Gwie, D.S., Saunders, C.M. & and Lauck, T.W. (2002). *Lessons learned from large-scale tests of unbonded braced frame subassemblages*. 71st Annual Convention, Structural Engineers Association of California, Sacramento, California.

Muir, L.S. & Thornton, W.A. (2014). *Vertical bracing connections - analysis and design*. Chicago, IL: American Institute of Steel Construction.

NZS 3404. (1997). *Steel structures standard*, Wellington: Standards New Zealand.

Palmer, K.D. Roeder, C. W. & Lehman, D.E. (2016). *Connection design recommendations for Improved BRBF performance*. (AISC) Engineering Journal, First Quarter, 29-45.

Takeuchi, T., Ozaki, H., Matsui, R. & Sutcu, F. (2014). *Out-of-plane stability of buckling-restrained braces including moment transfer capacity*. Earthquake Engineering & Structural Dynamics, 43(6), 851-869.

Takeuchi, T., Matsui, R. & Mihara, S. (2016). *Out-of-plane stability assessment of buckling-restrained braces including connections with chevron configuration*. Earthquake Engineering & Structural Dynamics.

Thornton, W.A. (1984). *Bracing connections for heavy construction*. (AISC) Engineering Journal, Third Quarter, 139-148.

Tsai, K., Hsiao, P., Wang, K., Weng, Y., Lin, M., Lin, K. & Lin, S. (2008). *Pseudo-dynamic tests of a full-scale CFT/BRB frame-Part I: Specimen design, experiment and analysis*. Earthquake Engineering & Structural Dynamics, 37(7), 1081-1098.

Tsai, K. & Hsiao, P. (2008). *Pseudo-dynamic test of a full-scale CFT/BRB frame-Part II: Seismic performance of buckling-restrained braces and connections*. Earthquake Engineering & Structural Dynamics, 37(7), 1099-1115.

Uriz, P. & Mahin, S.A. (2008). *Toward earthquake-resistant design of Concentrically braced steel-frame structures*. (Technical Report PEER No. 2008/08), Berkeley, USA: Pacific Earthquake Engineering Research Center.

Whitmore, R.E. (1952). *Experimental investigation of stresses in gusset plates*. University of Tennessee, Knoxville: University of Tennessee Experiment Station Bulletin No. 16.

Yam, M.C.H. & Cheng, J.J.R. (2002). *Behavior and design of gusset plate connections in compression*. Journal of Constructional Steel Research, 58(5–8), 1143-1159.

Example 1. NLYL Method for CBF Specimen No. 1 (Gross, 1990)

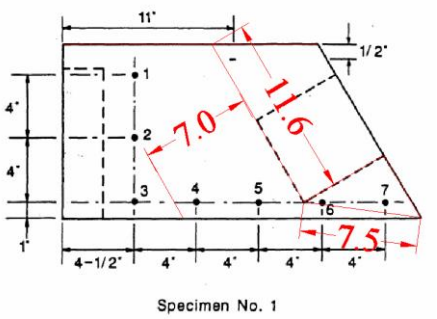

Figure 9. Specimen No. 1 (Gross 1990)

$F_y = 46.7\ ksi\ (322\ MPa)$

$t_g = 0.25\ in\ (6.35\ mm)$

$N = \theta_i N^\star = 0.022\ N^\star$

$b_{ga} = [2 \times tan(40^\circ) \times 4] + 3 = 9.71\ in\ (247\ mm)$

$A_g = t_g b_{ga} = 0.25 \times 9.71 = 2.43\ in^2\ (1566\ mm^2)$

$$L_{ave} = min \begin{cases} (a+c)/2 = (7+1)/2 = 4\ in\ (101.6\ mm) \\ (a+b+c)/3 = (7+12.5+1)/3 = 6.83\ in\ (173.5\ mm) \end{cases}$$

$b_{gf} = b_1 + b_2 = 7.5 + 11.6 = 19.1\ in\ (485\ mm)$

$$f_e = \frac{\pi^2 E}{\left(\frac{L_{ave}}{r_g}\right)^2} = \frac{\pi^2 \times 2 \times 10^5}{\left(\frac{101.6}{1.833}\right)^2} = 642\ Mpa$$

$N_e = f_e A_g = 642 \times 1566 = 1005\ kN$

$$\delta_S = \frac{1}{1 - \frac{N^\star}{N_e}} = \frac{1}{1 - \frac{N^\star}{1005}}$$

$$M_y^\star = \frac{N L_{ave} \delta_S}{2} = \frac{0.022 \times N^\star \times 101.6}{2} \times \frac{1}{1 - \frac{N^\star}{1005}}$$

$$S_g = \frac{b_{gf}\ t_g^2}{4} = \frac{485 \times 6.35^2}{4} = 4889\ mm^3$$

$$\left(\frac{N^\star}{N_s^g}\right)^2 + \frac{M_y^\star}{M_{sy}^g} \le 1 \Rightarrow \left(\frac{N^\star}{1566 \times 322}\right)^2 + \frac{0.022 \times N^\star \times 101.6}{2 \times \left(1 - \frac{N^\star}{1005 \times 10^3}\right) \times 322 \times 4889} \le 1$$

$$\rightarrow {N^\star}_{max} = 380\ kN$$

Example 2. NLYL Method for BRBs Specimen MRL2.0S1 (Takeuchi et al. 2014)

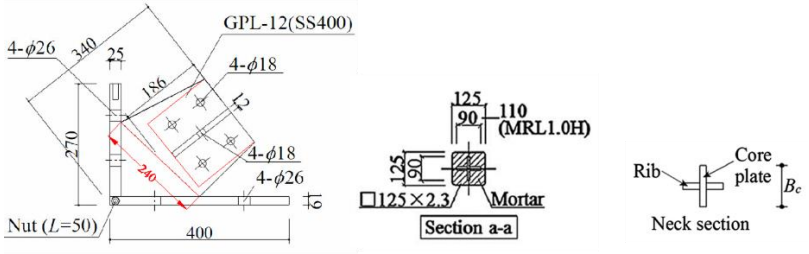

Figure 10. Specimen MRL2.0S1 (Takeuchi et al. 2014)

First assume plastic hinge location at the neck:

$$M_p^g = M_{sy}^g\left(1-\left(\frac{N_{cu}^\star}{N_s^g}\right)^2\right) \qquad M_p^{r-neck} = M_{sy}^n\left(1-\left(\frac{N_{cu}^\star - N_{wy}^n}{N_y^n - N_{wy}^n}\right)^2\right)$$

$$\theta_i = \frac{a_r}{\xi L_0} = \frac{6.8}{416} = 0.0163 \qquad N_{wy}^n = (B_c - t_R)(t_c)(f_y) = (78)(12)(266.8) = 250\ kN$$

$$N_y^n = [B_c t_c + (B_R - t_c)(t_R)] \times f_y = \left[(90)(12) + (90-12)(12)\right] \times 266.8 = 537.9\ kN$$

$$N_s^g = t_g b_{ga} f_y = \frac{(12)(240)(266.8)}{1000} = 768.4\ kN$$

$$M_{sy}^g = S_g f_y = \frac{b_{gf} t_g^2}{4} f_y = \frac{(240)(12)^2}{4}\ (266.8) = 2.305\ kNm$$

$$M_{sy}^n = S_n f_y = \left(\frac{(12)(90)^2}{4} + \frac{(78)(12)^2}{4}\right)(266.8)(10)^{-6} = 7.23\ kNm$$

$$N_{cr}^B = \frac{\pi^2 E I_B}{(kL_0)^2} = \frac{(\pi)^2(5.81)(10)^{11}}{(1\times 2392)^2} = 1002\ kN$$

$$N\xi L_0 \delta_S \le (1-2\xi)\, M_p^g + M_p^{r-neck}$$

$$(0.0163)(N_{cu}^\star)(0.416)\left(\frac{1}{1-\frac{N_{cu}^\star}{1002}}\right) \le (0.652)\left(1-\left(\frac{N_{cu}^\star}{768.4}\right)^2\right)(2.305) + \left(1-\left(\frac{N_{cu}^\star - 250}{537.9-250}\right)^2\right)(7.23)$$

$$\Longrightarrow N_{cu\,(max)}^\star \le 436\ kN \longrightarrow M_p^{r-neck} = 4.21\ kNm$$

Assume plastic hinge location at the restrainer end (Takeuchi et al. 2014):

$$M_p^{r-rest} = min\{S_{rp}\sigma_{ry};\ \alpha_p^r[K_{Rr1}\theta_{y1}' + K_{R2}(\theta_{y2} - \theta_{y1}')]\} \qquad S_{rp}\sigma_{ry} = (51947)(385.8)$$
$$= 20.04\ kNm$$

$$\alpha_p^r = 4.5 - 1.5(L_{in}/B_c) = 4.5 - 1.5(180/90) = 1.5$$

$$a = \frac{B_r - B_c}{4} = \frac{125-90}{4} = 8.75\ mm$$

$$K_{Rr1} = \frac{E B_r t_r^3 L_{in}^3}{3(2B_r a^3 - 3a^4)} = \frac{(2.05\times 10^5)(125)(2.3)^3\,(180)^3}{3(2\times 125\times 8.75^3 - 3\times 8.75^4)} = 4043490617$$

$$\theta_{y1}' = 1.64\times 10^{-3}(\sigma_{ry}/E)(B_r/t_r)(B_c/L_{in})$$

$$= 1.64\times 10^{-3}(385.8/(2.05\times 10^5))(125/2.3)(90/180) = 8.387\times 10^{-5}$$

$$K_{R2} = 0.11\sigma_{ry} B_r^3 (L_{in}/B_c)^3 = 0.11(385.8)(125)^3(180/90)^3 = 663093750$$

$$\theta_{y2} = \frac{B_r}{L_{in}}\sqrt{\left(\frac{\sigma_{ry}}{2E}\right)^2 + \left(\frac{a\sigma_{ry}}{B_r E}\right)} = \frac{125}{180}\sqrt{\left(\frac{385.8}{2(2.05\times 10^5)}\right)^2 + \left(\frac{8.75(385.8)}{125(2.05\times 10^5)}\right)} = 7.997\times 10^{-3}$$

$$\Longrightarrow M_p^{r-rest} = 8.38\ kNm \longrightarrow N_{cu\,(max)}^\star \le 572\ kN$$